THE RIKEN LINEAR ACCELERATOR - CYCLOTRON SYSTEM

H. KAMITSUBO
The Institute of Physical and Chemical Research
Wako-shi, Saitama 351, Japan

Summary

Present status of the RIKEN linear accelerator-cyclotron system is reported. The first injector is a variable-frequency linear accelerator which was completed in 1980. Construction of a separated sector cyclotron is in progress. Fabrication of four sector magnets was already finished and they are under installation at the Institute. Design of remaining parts of the SSC is almost finished and is outlined in this report.

1. Introduction

The RIKEN Linear Accelerator-Cyclotron System is the principal facility in the heavy-ion research program at the Institute of Physical and Chemical Research(RIKEN)[1]. The linear accelerator(RILAC), which is the first injector for the separated sector Cyclotron(SSC)with K-value of 540 MeV, was completed in 1980 and has been used for studies of atomic and solid state physics, material engineering, chemistry, radiation biology and so on. Details of the RILAC and its performance will be reported in this Conference by M. Kase[2].

Construction of the SSC started in 1981 and will be finished in 1986. All of four sector magnets were already completed at the factory and are under installation in the cyclotron vault. Preliminary measurement of the field distribution and excitation characteristics was done at the factory and beam dynamical calculations were performed using the results. Design of the remianing parts of the SSC was nearly finished and some of them were ordered to the company. A computer network system will be used for control of the SSC together with CAMAC interface. Prototype of the interfaces were made and tested.

After completion of the SSC in 1986 an AVF cyclotron will be built as the second injector for lighter ions of higher energies. Development of an ECR ion source is in progress. In Table 1 are listed the maximum energies for ions with a charge state q_i and mass number A_i when they are injected from the RILAC and the AVF cyclotron. Here q_i is the charge state of ions at the ion source of the injectors.

Table 1. Maximum Energy per Nucleon of RIKEN SSC

Injected from RILAC		
Ions with $A_i/q_i < 5$	70	MeV/u
Ions with $A_i/q_i \geq 5$	$(280 \sim 324) \times (q_i/A_i)$	MeV/u*
Injected from AVF Cyclotron		
Proton	210	MeV
^{3}He	185	MeV/u
Ions with $A_i/q_i = 2$	135	MeV/u
Ions with $A_i/q_i > 2$	$(1215 \sim 1102) \times (q_i/A_i)^2$	MeV/u*

* left and right numbers correspond to values for light and heavy ions,respectively

2. Coupling of the RILAC and the SSC

The RILAC is the first variable-frequency linear accelerator which was brought into operation in the world and is suitable for an injector to cyclotron. Coupling of the RILAC and the SSC can be realized when following matching conditions are fulfilled: Path length of the first equilibrium orbit in the SSC is to be equal to an integral multiple of effective length of the last drift tube of the RILAC. Secondly the frequency of accelerating voltage of the SSC is also an integral multiple of the RILAC frequency if all the ions from the RILAC are to be accepted by the SSC. From the first condition the mean injection radius and the harmonic number were determined to be 0.89 m and 9, respectively. As for the second condition we decided the frequency of the RF system is equal for both the RILAC and the SSC. The effective angle of an accelerating electrode (Dee) must be 20 degree or an angle close to that. Taking into account the matching with the injector cyclotron, we adopted the dee angle of 23.5 degree.

Because the frequency range of the RILAC is from 17 to 45 MHz, the RF system of the SSC must work well in this frequency range. During design work of the SSC resonator it became clear that RF voltage distribution along the accelerating gap of the dee has an minimum in the middle in radial position. However the beam dynamical calculations showed a radially increasing distribution is indispensable for getting a beam of good quality. As described later we could realize the radially increasing distributions over a whole frequency range if we abandon a frequency region lower than 20 MHz. On the other hand, it was found that beam energy of the RILAC can be changed very easily in a wide range by changing only the RF phase of the last cavity.[2] Then it is possible to accelerate ions at lower energy in the SSC by changing the harmonic number from 9 to 10 or 11 without changing the frequency of both RILAC and SSC. This means that even if we narrow the frequency range we can cover the same energy range as in the case that the frequency range is from 17 to 45 MHz. Thus we finally atopt the frequency range from 20 to 45 MHz for the RF system of the SSC.

Beam lines of the RILAC and the SSC are not in the same level and difference in height is 12 m[1]. The beam from the RILAC should be transported horizontally as well as vertically by about 40 m. Matching of the beam emittance in six dimensions to the acceptance of the SSC is realized by the transport system between the RILAC and the SSC[3].

CH1996-3/84/0000-0257 $1.00 © 1984 IEEE

Table 2.Principal Parameters of RIKEN SSC

Number of Sector Magnets	4
Sector Angle	50°
Gap Width	8 cm
Maximum Magnetic Field	1.55 T
Maximum Magnetomotive force	1.35×10^5 AT
Maximum Current	1000 A
Current Stability	0.002 %
Maximum Power	700 kW
Total Weight	2100 ton
Number of Trim Coils	29 x 4 pairs
Maximum Current	500 A
Current Stability	0.05 %
Total Trim Coil Power	200 kW
Number of Dees	2
Dee Angle	23.5°
RF Range	20 - 45 MHz
RF Tuning Device	Movable Box and Trimming
Maximum RF Voltage	250 kV
Maximum RF Power	600 kW
Main Evacuation System	10^4 ℓ/sec Cryopumps
Pressure	$< 1 \times 10^{-7}$ Torr.
Controle System	Computer Network and CAMAC Interface
Dimension of the SSC	
Diameter	12.6 m
Height	6 m
Mean Injection Radius	0.893 m
Mean Extraction Radius	3.56 m
Orbit Frequency	1.9 - 7.37 MHz
Harmonic Number	
Injected from RILAC	9
Injected from AVF	5

In due course the harmonic number of the SSC for a beam injected from the AVF cyclotron is changed from 6 to 5. The mean extraction radius of the AVF cyclotron becomes 0.75 m, that is, 5/6 of the mean injection radius of the SSC.

Development of the ECR ion sources both for the RILAC and the SSC is in progress. As can be seen in Table 1, the new sources can expand the maximum energy of heavier ions.

Reviced principal parameters and specifications of the SSC are listed in Table 2.

3. Sector Magnets

A plan view of the SSC is shown in Fig. 1. The SSC is composed of four sector magnets, two RF resonators, two vacuum chambers,injection and extraction elements and beam diagnostic devices. The sector magnets should produce magnetic field in a range from 0.7 to 1.55 T. The field has a distribution needed for focussing and orbit stability of the beam and for satisfying isochronism in a wide range of energy and ion mass. The yoke is made of rolled steel of low carbon content (0.04 %) and divided into 28 slabs for the convenience of transportation from the factory. Ratio of a cross-sectional area to a pole base area is 0.94 which is the minimum allowable value to achieve the required field strength.

The pole is made of homogeniously forged steel with carbon content of 0.01 %. Radial edges of the pole have a profile of an approximated B-constant

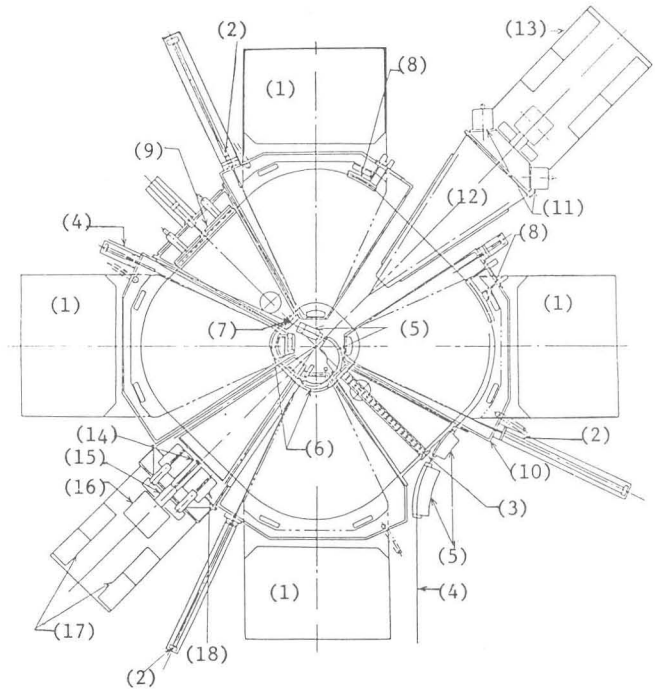

(1) Sector Magnet
(2) Beam Probe
(3) Phase Probe
(4) Beam Line
(5) Bending Magnet
(6) Magnetic Inflection Channel
(7) Electric Inflection Channel
(8) Magnetic Deflection Channel
(9) Electric Deflection Channel
(10) Vacuum Chamber
(11) Vacuum Pump
(12) Resonator
(13) Platform Car
(14) Coupler
(15) Feeder Line
(16) Final Amplifier
(17) DC Power Supply & Controle Panel
(18) Trimmer

Fig.1 A Plan View of RIKEN SSC

shape. A flange for a vacuum chamber is welded on the pole side. Twenty nine trim coils are directly mounted on the pole face. Each of trim coils is made of copper plate of 6 mm thick and has a curved shape along the equilibrium orbit. Its radial width and position were determined from the optimization calculations using the field distribution calcualted by TRIM code[4]. A hollow conductor is welded to the copper plate to feed DC current and cooling water. For narrow trim coils, only hollow conductors with curved shape are used. Both copper plate and hollow conductor

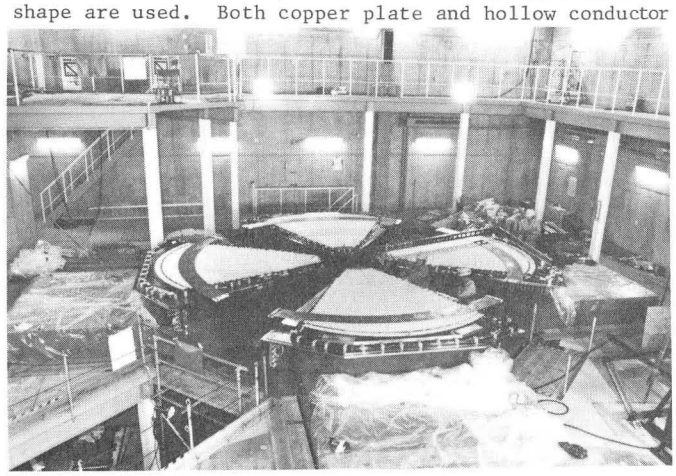

Fig. 2. A photograph of the sector magnets which are under installation in the cyclotron vault.

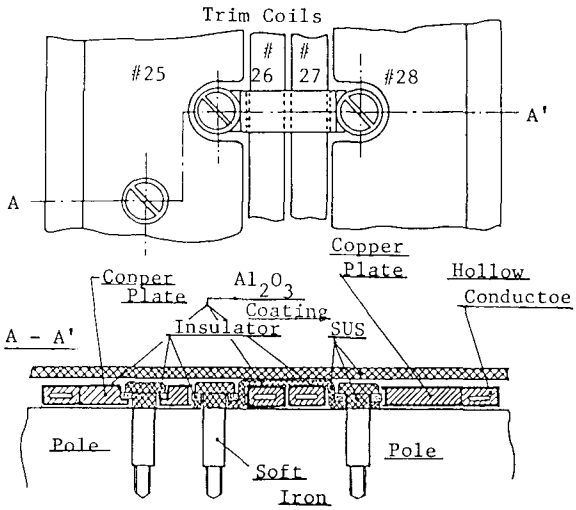

Fig. 3 Mounting of trim coils on the pole face

are flash-coated with Al_2O_3 for electric insulation. Fig. 2 shows a photograph of the sector magnets which are under installation in the cyclotron vault. Trim coils and a flange for the vacuum chamber can be seen clearly in the photograph. Three spacers will be put, one is at the center portion and the other two are along the outer edge of the pole. Because Al_2O_3 coating will adsorb a large amount of gas and bad for high vacuum, trim coils as well as pole faces are separated from the main vacuum chamber and are kept under low vacuum. Fig. 3 shows details of trim coil mounting and stainless steel plate which separates high and low vacuum parts. The trim coils are fixed on the pole face with bolts which were made specially for this purpose. As can be seen in the figure, a part screwed inside the pole is made of soft iron whereas a part remained outside of the pole is made of stainless steel. Thus field disturbance due to bolts and their holes can be reduced considerably.

Fabrication of the sector magnets started in 1981. Excitation characteristics and field distributions were measured for the first magnet in March, 1982 and then preliminary measurement of field distribution for use of orbit calculations were carried out after installing the first and second magnets at the factory[5]. Magnetic field produced by each trim coil was also measured and the results were used for development of program for trim coil current optimization to produce

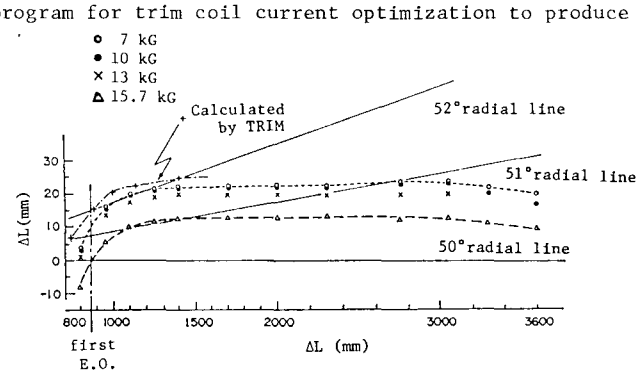

FIG. 4 Change of effective field boundaries obtained from the measurement at the positions along the sector edge line. The measurement was made at the fields of 7, 10, 13, and 15.7 kG (○, ●, ×, △). The calculated effective field boundaries in the nose region (+) are also shown. ΔL: Position of effective boundary measured from 50° radial line. R: Radial position along 50° radial line.

the isochronous field distribution. A typical result of the measurements are shown in Fig. 4 where effective feild boundaries obtained from field distribution measurements at the field of 0.7, 1.0, 1.3 and 1.57 T are plotted along the sector edge line.

All the sector magnets were completed and are under installation at RIKEN. Power supplies for the main and trim coils will be delivered in July and field measurement will restart in September of this year.

4. RF System

We reported previously that a vertical half-wavelength coaxial resonator was investigated as a candidate for the RF system of the SSC[1]. In the middle of the resonator corresponding to the widest part of the wave it has a delta-shaped dee which is supported by two vertical stems on the upper and lower sides. For a frequency changing device two were investigated so far. One is a movable shorting plate and another is a movable box. Although the former has a merit of having a high Q-value, it has a demerit that total height of the resonator is large (7 m) and therefore travelling distance of the shorting plate is long (2m). It has also difficulty that current density at the contact fingers of the shorting plate is very high. On the other hand the latter seemed very promising because total height of the system can be reduced considerably and also current density at the contact fingers of the movable box is smaller than that of the shorting plate. Thus we decided finally to adopt the resonator with two movable boxes on the upper and lower sides. In the early stage of designing the vertical stems turned at the position of about one thirds of their length to forward direction or direction of small radius. This structure was adopted to improve the voltage distribution along dee gap. However, as mentioned in Sec. 2, it became clear that the frequency range can be narrowed so that we could make stem length shorter. Then it is possible to adopt the straight stem and realize the radially increasing voltage distribution easily[6]. Fig. 5 shows a bird's-eye view of the new RF resonator. Total height of the present resonator is 2.1 m and travelling distance of the box is 0.7 m. RF power will be feeded through a coupler. Fine tuning of the frequency can be done using a trimmer. The trimmer

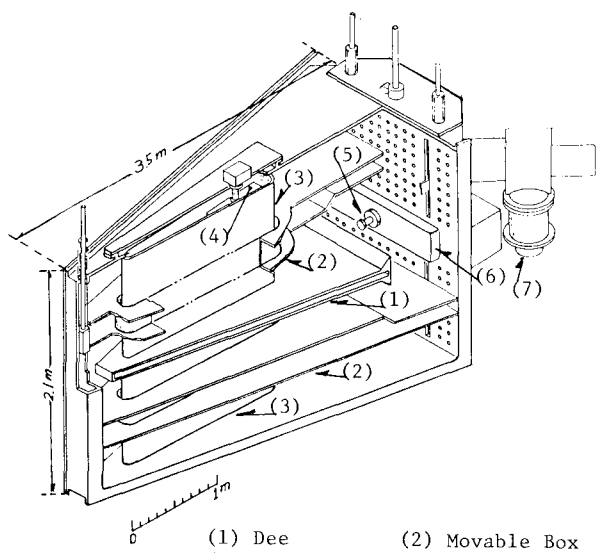

(1) Dee (2) Movable Box
(3) Stem (4) Cryopanel
(5) Coupler (6) Trimmer
(7) Vacuum Pump

Fig.5 A bird's-eye view of the RF Resonator for the SSC

and the coupler are inserted from the backside. The backside plate is made of copper cladded stainless steel and has many small holes for evacuation. Behind the plate is a vacuum chamber of the resonator and two cryopumps and a turbomolecular pump will be equipped to it. A cryopanel will be put inside of the stem to evacuate inside of the dee.

Estimated Q-values and resonant frequencies are shown in Fig. 6 as a function of the movable box position measured from the median plane. When the box is close to the dee, capacitance between the box and the dee is large and the Q-value decreases in low frequency region. In general RF voltage required for turn separation large enough to extract the beam with high efficiency is lower in low frequency region than in high frequency region. Fig. 6 shows a relation between RF voltage and frequency for the present resonator. The solid lines correspond to the RF voltage at different input power. The broken lines show the RF voltage needed to realize 8 mm turn separation at the extraction radius for ions with mass to charge ratio given by numbers on the lines. From this calculation the maximum output power of the final stage amplifier is required to be larger than 250 kW. Preliminary calculations showed that RF voltage distribution along the accelerating gap is radially increaing over whole frequency range. Measurement of the static characteristics on the one fourth model will be done in near future.

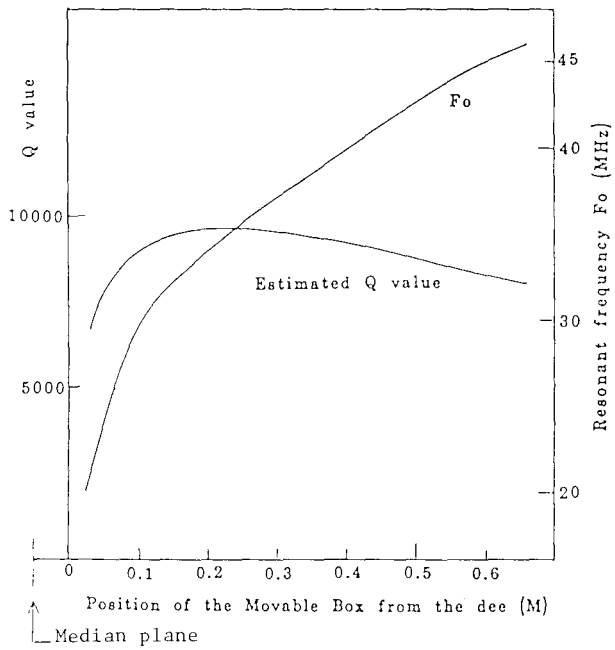

Fig.6 Resonant frequency and Q-value of the resonator with the movable box

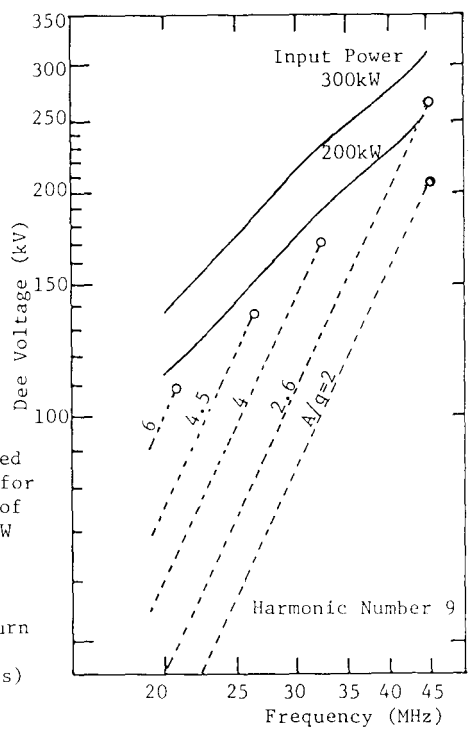

Fig.7 Estimated dee voltage for input power of 200 and 300kW (solid line) and required values for sufficient turn separation (broken lines)

Master oscillater and power amplifier system is to be employed for a RF oscillator system. Synchronous operation with the RF systems of the injectors is necessary in a wide range of frequency. High stability of RF voltage as well as its phase is also required. The maximum output power is larger than 250 kW as mentioned before. An RCA 4648 tetrode will be used for the final amplifier. Fig. 8 shows a cross-sectional view of the final stage amplifier and its tuning circuit. A center conductor of the plate stub is a copper pipe of 18 cm in diameter and a outer conductor as well as an internal box above DC blocking capacitor of the plate circuit are square boxes made of alminum. Cooling water pipes and a DC power line for the tube are to pass through the inside of the center conductor in the stub. The internal box is also useful to accommodate joints for water pipes and other equipments. It helps to shorten the length of the stub at low frequency. In designing of the power amplifier using RCA 4648 tube, it was found that capacitive coupling between the

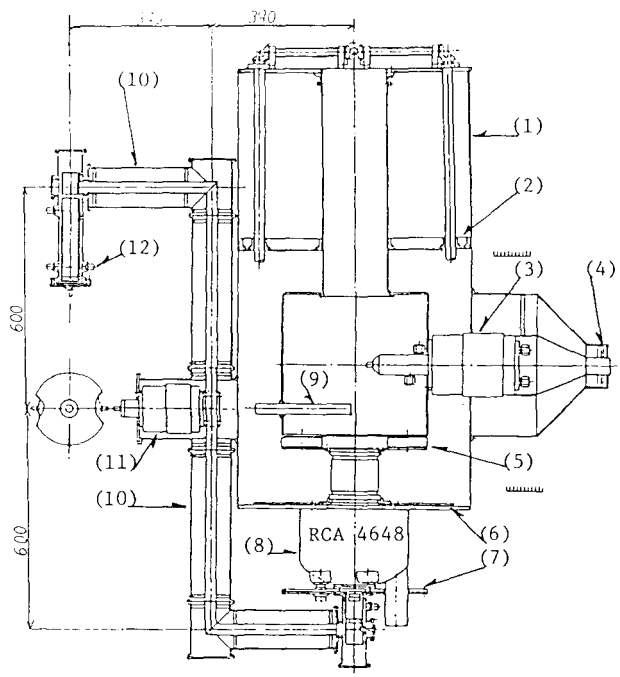

(1) Plate stub,81Ω (2) Movable short
(3) Impeadance matching capacitor
(4) Feeder line (5) Plate DC blocking capacitor
(6) Screen bypass capacitor
(7) Cathod bypass capacitor (8) Tube
(9) Neutralization electrode
(10) Grid tuning coaxial line, 74Ω, 0.9m
(11) Grid tuning capacitor (12) Input

Fig. 8 Cross-sectional view of the power amplifier stage

plate and the grid in the tube gave serious instability at high frequency. A method to neutrize this effect was developed[7)]

5. Vacuum System

The vacuum chamber of the SSC is divided into eight sections, that is, four magnets chambers, two RF resonator chambers and two valley chambers (Fig.1). Because of very limited space in the central region, it is quite difficult to apply usual metal seals so that elastomer and expansion sealing will be used between the chambers. The pressure in the chambers must be kept low in order to reduce beam loss due to ion scattering by residual gas molecules as low as possible. If the beam loss is to be kept less than 10 %, the pressure inside the chamber must be lower than 10^{-7} Torr. From the preliminary design of the SSC we can estimate total volume of the vacuum chamber to be $30m^3$ and its inside surface area 350 m^2. Then total outgassing rate can be estimated as 7.7×10^{-3} Torr·ℓ/sec. An additional gas load of about 3×10^{-3} Torr·ℓ/sec will be caused by evolution from various components inserted in the vacuum and also by permeation through the sealing elastomer[8)]. Then the total pumping speed of 12×10^4 /sec. is required to achieve a pressure lower than 1×10^{-7} Torr inside the chamber. To guarantee this pumping speed, ten cryo-pumps with speed of 10,000ℓ/sec. and four turbo-molecular pumps will be equipped to the chamber.

As mentioned in Sec.3, trim coils are coated with Al_2O_3 which adsorb large amount of gas. To reduce this effect trim coils and poles are covered with stainless steel plate of 4 mm thick and kept under low vacuum. Fig. 9 shows a cross-sectional view of pole edge section.

In order to reduce the gas load as low as possible, discharge cleaning technique is to be applied to the magnet chambers. Because in these chambers it is easy to apply magnetic field needed to the electron cyclotron resonance(ECR). Then it is possible to apply ECR discharge cleaning for degassing. An experimental apparatus for ECR discharge cleaning was built at the model magnet of the old cyclotron and tested. The results showed that the impurity molecules of about 7.2×10^{18} were transformed from the surface into gas and thus the surface was cleaned considerably[9)].

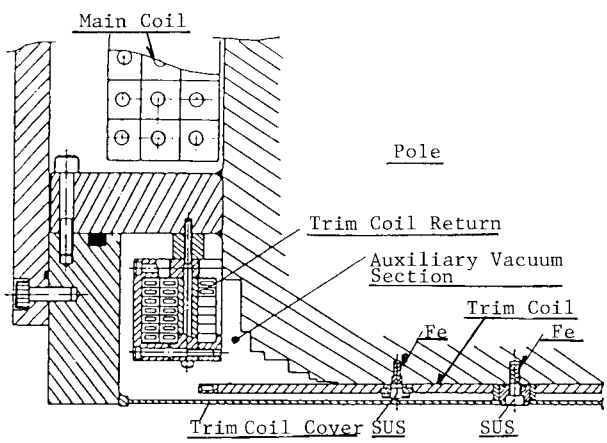

Fig. 9 Cross-sectional view of the pole edge section. Pole surface and trim coils are enclosed in auxiliary vacuum and separated from high vacuum chambers. The main coils are in the atomosphere.

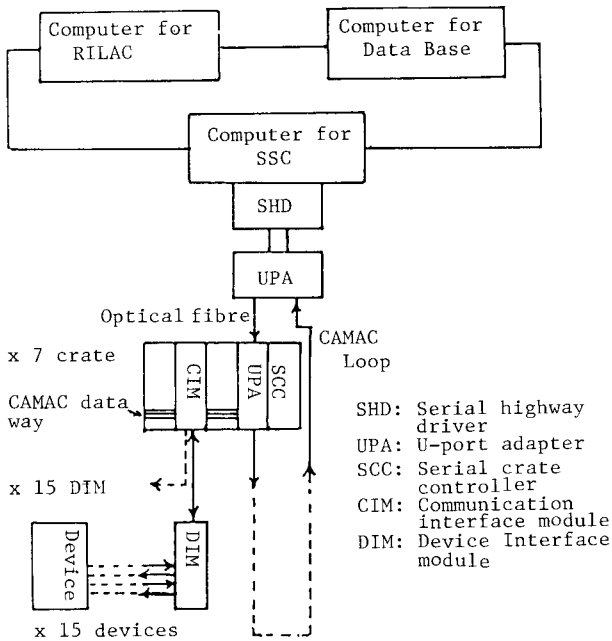

Fig. 10 Schematic diagram of the controle system.

Three types of one-third scale model of the pneumatic expansion seal were made and their performance was investigated. Numerical analysis of deformation of the seal was also done using the finite element method. Design of the evacuation system is finished.

6. Controle System

A computer aided controle system will be introduced for the SSC. The system is composed of a network of three computers and CAMAC system. The computer is MELCOM350-60/500 and its word length is 32 bits. Among them one is used for control of the SSC, the second for control of the RILAC and the last will be used for program development and data file. These three computers are equivalent and can be supported by each other through the network. Fig. 10 shows a schematic diagram of computers and CAMAC system. In the control system of the RILAC used the GP-IB system.

All the devices will be controled through the CAMAC by the computer. To decrease necessary number of CAMAC crates, modules and signal cables, new CAMAC modules named CIM(Communication Interface Module) and DIM(Device Interface Module) are developed. They have the following functions: 1) Execution of macro-programs for a seaquetical control and a data acquisition. 2) Periodic logging and storage of status information independently from the computer. 3) Block transfer of information from/to the control computer. 4) Automatic alarm to the control computer at an apparatus failure. These intelligent interface modules can control the devices locally and ensure high speed sequential control and measurements without any aid of the control computer.

The CIM consisits of CPU, ROM and RAM commonly connected to the internal bus. Programs for monitor and various tasks are stored in ROM whereas apparatus information and data are stored in RAM. Programs and data downloaded from the control computer are also stored in RAM. The CIM can be linked with sixteen DIM's.

The DIM has also CPU, RAM and ROM which are connected to the common bus inside the DIM.

CH1996-3/84/0000-0261 $1.00 © 1984 IEEE

In addition it has sixteen output ports buffered by resistered and sixteen input ports with gates. These input and output ports are connected directly with devices to be controled or through optional elements such as D/A or A/D converters. However two of the input ports will be used for fetching status information of apparatus. Instructions and data between CIM and DIM are transmitted through Receiver/Transmitter equipped to the CIM and DIM and optical fibre. Prototypes of the CIM and DIM were made and their tests are in progress[10].

7. Beam Transport System and Experimental Rooms

This facility will be devoted to research works in various fields such as nuclear and atomic physics, solid state physics, material engineering, nuclear and radiation chemistry and biomedical study. Frequent change of energy and ion species will be expected and required beam quality as well as intensity will diverge widely. In designing the beam transport system these requirements must be taken into account. The main feature of the beam transport system is that double telescopic two 90° bending magnets system is used. All the elements are arranged as symmetric as possible[11]. Layout of the beam transport lines and the experimental rooms for various research fields is shown in Fig. 11. The following functions can be fulfilled in a practical sense:

(1) Achromatic and double-telescopic transport.
(2) Isochronous, non-dispersive and double-telescopic transport with a time resolution less than 500 ps.
(3) Monochromatic and double-telescopic transport with a momentum resolution up to 20,000.

The first mode is available at every target area. The second mode is available at Lab.4 and 6. In mode (1) or (2) the momentum resolution of about 10,000(0.02% energy resolution) is achieved by using the first bending magnet B_1. The third one is a double-dispersive transport to Lab. 2,3 and 6. By taking into account the second order aberration, the momentum resolution was estimated to be 20,253 for a beam whose maximum horizontal divergence is 2.432 mrad at the object point S_0. The slit width at S_0 is assumed to be 1 mm. Biomedical studies will be done in Lab. 5 by using heavy ion beam and a possibility to use protons and alpha particles for radiotherapy of cancer is discussed.

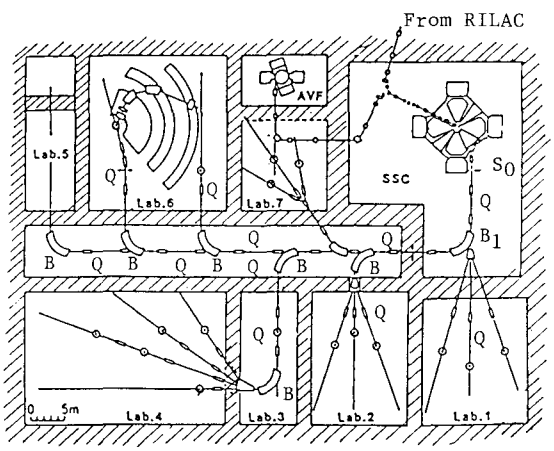

Fig.11 A plan view of the beam handling system and layout of the experimental rooms. S_0 is the object point of the system.

8. Time Schedule

Construction of the RF system, vacuum chamber and evacuation system, beam injection and extraction system and beam diagnostic system will be ordered to the manufacturerer in May. The SSC will be completed in the summer of 1986. The beam transport system after the SSC will be constructed from next year. We expect the first trial of beam injection from the RILAC will start in the autumn of 1986. The second injector or an AVF cyclotron will be constructed from 1987.

9. References

1. H. Kamitsubo, Proc. of 9th Intern. Conf. on Cyclotrons and their Applications, Caen (1981) 13
2. M. Kase et al, this Conferernce
3. N.Kishida and Y. Yano, Sci. Papers I.P.C.R.(RIKEN) 75 (1981) 214
4. A.Goto,H.Takebe,S. Motonaga,Y.Yano, N. Nakanishi and T.Wada, Sci. Papers I.P.C.R.(RIKEN) 77(1983)54
5. S. Motonaga, H. Takebe, A. Goto, Y. Yano, T. Wada and H. Kamitsubo, J. de Physique C1(1984) 213
6. T. Fujisawa, K. Ogiwara, S. Kohara, Y. Oikawa, I. Yokoyama, M. Hara, I. Takeshita and Y. Chiba, this Conference
7. S. Kohara and T. Fujisawa, RIKEN Accel. Prog. Report 16 (1982) 173
8. S. Nakajima, K. Ikegami, Y. Oikawa and I. Takeshita, Proc. 4th Symp. on Accelerator Science and Technology, Saitama (1982) 203
9. K. Ikegami, S. Nakajima, Y. Oikawa, Y. Ishibe, H. Ohyama, Y. Sakamoto, S. Motonaga and H. Kamitsubo, Sci. Papers I.P.C.R.(RIKEN) 77 (1983)78
10. K. Shimizu, T. Wada, J. Fujita and I. Yokoyama, this Conference
11. T. Inamura, N. Kishida, H. Saito and M. Watanabe, Sci. Papers I.P.C.R.(RIKEN) 75 (1981) 326